Colloid Polym Sci (2008) 286:1215–1222
DOI 10.1007/s00396-008-1901-3

ORIGINAL CONTRIBUTION

Sealed and temperature-controlled sample cell for inverted and confocal microscopes and fluorescence correlation spectroscopy

Claus B. Müller · Walter Richtering

Received: 30 April 2008 / Revised: 9 June 2008 / Accepted: 11 June 2008 / Published online: 13 July 2008

Abstract Precise temperature control of sample environments plays a key role while exploring biological systems or temperature-sensitive materials. We have developed a sample cell for inverted microscopes, which allows a temperature accuracy of ±0.05 K in a temperature range of 5 to 65 °C, with an absolute precession of ±0.1 K. Our sample cell is developed for requirements of single-molecule experiments, which comprises easy-to-clean and well-sealed devices to prevent solvent evaporation. The applied control algorithm permits a tunable independent setting of heat and cooling behavior and allows the application on microscopes without any objective heating. For measuring precise and absolute diffusion coefficients with two-focus fluorescence correlation spectroscopy, the exact control of the sample temperature is essential. We performed diffusion measurements of TetraSpeck 100-nm fluorescent latex particles and of temperature-sensitive microgels in aqueous solutions to demonstrate the excellent temperature stability and reproducibility of the device.

Keywords Temperature control · Sample cell · Absolute diffusion coefficients · Temperature-sensitive microgel · Hydrodynamic radius · Dual-focus FCS · 2fFCS · Confocal microscope

Introduction

The novel technique of two-focus fluorescence correlation spectroscopy (2fFCS) [1] opens the field for accurate determination of diffusion coefficients of small molecules, polymers, and colloidal particles. Most important for diffusion measurements in liquids is the precise control of sample temperature, as solvent viscosity also has strong temperature dependence [2].

By reviewing literature on fluorescence correlation spectroscopy (FCS) [3], established in the 1970s, it may be mentioned that since then most experiments were performed at room temperature, e.g., in a recent publication [4], by measuring diffusion coefficients of rhodamin 6G, which is used since 30 years ago as calibration standard for FCS.

In aqueous solution, the temperature change from 25.0 to 26.0 °C decreases the viscosity of the solvent, leading to an increased diffusion coefficient of 2.57%, which is in the order of magnitude of the overall precession of 2fFCS experiments [5] (accuracy typically better than 2%). Therefore, temperature determination and its constancy in the sample should be much better than 1.0 K.

Confocal laser scanning microscopy is often employed to investigate packing of particles in colloidal glasses and crystals. Recently, there is an increased interest in the crystallization behavior of temperature-sensitive microgel particles [6–10]. In addition, FCS is increasingly employed to investigate self-assembly in colloidal and polymer solutions [11–14]. Temperature-dependent FCS measurements can provide important new information on the self-assembly of multifunctional polymers and colloids [15–18].

Surprisingly, there are currently no sealed and temperature-controlled sample cells for inverted microscopes available. When developing a temperature controller, regulation accuracy better than ±0.1 K should be aimed for. The most challenging point in developing a suitable temperature cell is the water immersion objective, which is

C. B. Müller · W. Richtering (✉)
Institute of Physical Chemistry, RWTH Aachen University,
52056 Aachen, Germany
e-mail: richtering@rwth-aachen.de

often used in confocal microscopy setups. The thin water film between the sample and the objective establishes a thermal bridge; hence, in the ideal case, the objective and sample must have the same temperature.

In the case of our 2fFCS system "Micro Time 200" (PicoQuant, Germany), which is available with special confocal imaging options like "objective scanning", the whole microscope objective is moved in three dimensions with piezo scanners type P-720 (PIFOC) and P-733 (PI, Germany). A confocal image is generated by stepwise and as fast as possible complete scanning of the sample. For a picture with 512×512 pixels, almost a quarter of a million acceleration and deceleration steps are performed in a few minutes. Reduction of mass inertia of moved parts is a key for precise positioning control of the objective. Therefore, in a setup with objective scanning, it is not recommendable to connect the objective to a heat transducer, which would increase the mass inertia of the shifted objective. In consequence, exempt from room temperature, a strong initial temperature difference between sample and objective is expected. The sole possible way to solve this problem is the design of the sample cell itself.

The sample environment presented here satisfies the requirements of the highly sophisticated 2fFCS method and is also able to fit on inverted microscopes, which may be used for imaging and diffusion measurements in materials and life sciences.

Experiment

Two-focus fluorescence correlation spectroscopy

Starting with a confocal MicroTime 200 setup (PicoQuant, Germany), we have modified the microscope to introduce an *external length* scale into the measurement. The external length scale is created by two laterally shifted but overlapping foci with well-known and fixed distance (2fFCS) [1]. The autocorrelation function (ACF) for each focus is computed separately [19] as well as the cross-correlation function (CCF) of the fluorescence between both foci. The diffusion coefficient of the fluorescent molecules can be calculated absolutely and without reference by analyzing the delay of the CCF decay in comparison to the ACF decay (which is due to the extra distance between both foci). Although optical aberrations or saturation effects may distort the shape of the molecule detection function (MDF) of each focus, the distance between them and thus the intrinsic ruler used for the diffusion coefficient calculation is not changed by these effects. A detailed description of the instrument and calibration can be found in [20].

An important part of 2fFCS is the use of an appropriate model for the MDF, which relates the CCF to the diffusion coefficient:

$$\widetilde{g}(t,\delta,v) = \frac{c}{4}\sqrt{\frac{\pi}{Dt}} \times \int \mathrm{d}z_1 \int \mathrm{d}z_2 \frac{\kappa(z_1)\kappa(z_2)}{8Dt + w^2(z_1) + w^2(z_2)} \times \exp\left[-\frac{(z_2 - z_1 - v_2 t)^2}{4Dt} - 2\frac{(\delta - \mathrm{v_x}t)^2 + v_y^2 t^2}{8Dt + w^2(z_1) + w^2(z_2)}\right], \tag{1}$$

which has to be evaluated numerically [1]. Here, δ is the lateral distance between the foci, ε_1 and ε_2 are two factors proportional to the overall excitation intensity and detection efficiency in each laser, c is the concentration of the fluorescent molecules, and D is the diffusion coefficient. Here, the functions $\kappa(z)$ and $w(z)$ are given by:

$$w(z) = w_0\left[1 + \left(\frac{\lambda_{\mathrm{ex}} z}{\pi w_0^2 n}\right)^2\right]^{1/2} \tag{2}$$

and

$$\kappa(z) = 2\int_0^a \frac{\mathrm{d}\rho\rho}{R^2(z)} \exp\left(-\frac{2\rho^2}{R^2(z)}\right) = 1 - \exp\left(-\frac{2a^2}{R^2(z)}\right) \tag{3}$$

with

$$R(z) = R_0\left[1 + \left(\frac{\lambda_{\mathrm{em}} z}{\pi R_0^2 n}\right)^2\right]^{1/2} \tag{4}$$

where λ_{ex} and λ_{em} are the excitation and center emission wavelengths, respectively, n is the sample refractive index, a is the confocal pinhole radius, and w_0 and R_0 are fit parameters. According to the Stokes–Einstein equation [21]:

$$R_{\mathrm{h}} = \frac{k_{\mathrm{B}} T}{6\pi\eta D}, \tag{5}$$

where the hydrodynamic radius R_{h} is obtained from the measured diffusion coefficient D.

Dynamic light scattering

Dynamic light scattering (DLS) measurements were performed on a standard ALV 5000 system, equipped with laser (light wavelength 633 nm). Scattering intensity was detected at angles of 60°, 90°, and 120°, respectively, and the hydrodynamic radius was calculated with a second-order cumulant fit using the Stokes–Einstein relation. The measurement system was equipped with a temperature-controlled water bath giving a precision in sample temperature stabilization of ±0.2 K.

Investigated materials

For stability measurements, we used TetraSpeck 100 multi-fluorescent latex beads (TS 100) with a specified diameter of approximately 100 nm, which were purchased from Invitrogen (Karlsruhe, Germany) and used without any further purification. TS 100 particles consist, by the specification of the manufacturer, of continuously fluorescent-labeled spherical beads. The beads contain a mixture of four fluorescent dyes with well-separated excitation/emission peaks (365/430, 505/515, 560/580, and 660/680 nm). The width of the absorption peaks allows for a proper excitation with laser sources at 470, 532, and 632 nm. We have shown that R_h is equal to 56.6 nm [20]. In the current contribution, we have characterized the particles with the 633-nm laser pair.

PNIPAM^{Rhodamine} (poly-*n*-isopropylacrylamide) fluorescent-labeled microgel was synthesized following standard protocols as published in [6, 22–24], but with a mixture of unlabeled and labeled monomer (molar ratio approximately 1:0.016). The labeled monomer (methacryloxyethyl-thiocarbamoyl-rhodamine B, no. 23591) was purchased from Polysciences (400 Valley Road, Warrington, PA, USA). DLS and 2fFCS experiments were performed on the same sample concentration of 0.05 wt.% microgel solution. PNIPAM^{Rhodamine} was prepared in LiChrosolv water for chromatography (no. 115333), purchased from Merck KGaA (Darmstadt, Germany).

Apparatus description

For developing a suitable sample environment for 2fFCS experiments, we considered basic requirements which must be satisfied by the resulting sample cell. The sample should be completely sealed in the cell to prevent evaporation. Experiments with volatile organic solvents should also be possible as well as sample preparation outside measurement setup, e.g., under nitrogen conditions. Therefore, parts of the cell which have contact to the sample solution have to be made from inert material and the sample cell itself has to be portable from preparation places, like glove box, etc., to the 2fFCS instrument.

A typical advantage of single-molecule experiments on 2fFCS setups is the small size of detection volume (typically in femtoliters); hence, the sample amount can be kept as small as possible. Furthermore, single-molecule experiments make it essential to allow an easy and highly efficient cleaning protocol to prevent interference from molecules left from former experiments.

In addition, it is important for diffusion measurements that molecules to be investigated are not influenced by convection. Therefore, heat flow through the sample cell from and toward the microscope objective (especially in case of nontempered objective) should be guided around the sample volume and not through, in order to reduce the influence on temperature inside the sample.

Mechanics

The sample cell consists of three parts: the lower body, an inset, and the closing cap. The lower body with an outer diameter of 35 mm contains a Pt100 sensor, which is located close to the sample volume. The inset fixes the lower cover glass with a sealing ring to the body. The upper sealing ring is also mounted to the inset. Such cells can be handled easily under nitrogen conditions because, when sealing the sample inside, only the upper cover glass has to be put in before screwing the cap in the inset.

For sample cell material, we recommend stainless steel type 1.4571. Stainless steel of this type shows excellent inert properties against most chemicals and solvents. To clean the sample cell for fluorescent experiments, an irradiation with UV light can be performed, destroying any fluorescent molecules left; hence, only the inset has to be processed because this is the only part which is in direct contact to the sample. Pyrolytic cleaning under conditions up to 500–600 °C was also tried out successfully.

The lower body is shaped similar to the upper side of the microscope's objective but leaves a 2-mm gap to the objective, to use external immersion water supply, consisting of a syringe pump AL1000 (World Precision Instruments, Berlin, Germany) with a 50-ml syringe attached. To bring the immersion liquid to the objective, an intravenous catheter-type Surow-W 1.50× 45 mm (Terumo Europe N.V., Leuven, Belgium) is used. To prevent scratches on the objective, the inner injection needle is removed and only the outer perfluor-(ethylenepropylene-) plastic tube is attached onto the top of the objective.

To cover the sample, standard round microscope cover slips with a diameter of 10 and 22 mm are used for single utilization. Sealing rings made of Viton® are used with a dimension of 18×1 and 8×1 mm.

The diameter of the sample volume is smaller than the lens diameter of the objective. The outer metal body of the objective is connected via immersion liquid and the lower cover glass is connected to the metal part of the sample cell, providing a suitable way of heat flow around the sample volume itself. The distance between cover glasses is approximately 1.5 mm to form a sample reservoir, preventing convection. A detailed technical drawing is shown in Fig. 1. The sample cell is mounted with a Plexiglas® plate to the standard microscope table to decouple the sample cell from the metal body of the microscope.

The temperature stabilization of the sample cell is performed by an 18-W thermoelectric element (TEM), type TB-38-1,0-0,8CHR (Kryotherm, Saint-Petersburg, Russia). The backside of the TEM is equipped with a fluid heat

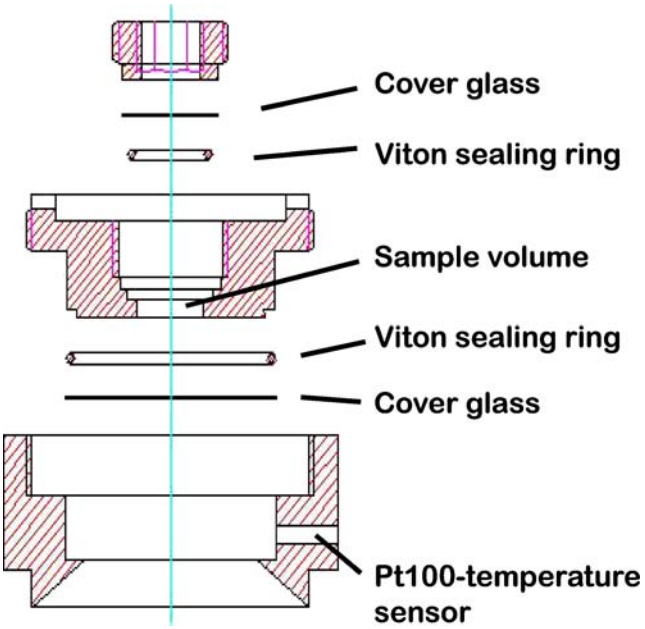

Fig. 1 Mechanical drawing of the sample cell made from stainless steel. The lower body is equipped with Pt100 temperature sensor. Sealing rings are mounted to inset

exchanger, which is adjusted to the temperature of the sample cell by an F30-C cryostat (JULABO Labortechnik, Seelbach, Germany). Thus, temperature is roughly tuned by the cryostat and thermal fluctuations are compensated by the TEM. The complete mounting of the temperature-controlled environment is shown in Fig. 2.

Electronics

The power controller for the TEM is developed for special requirements of the MicroTime200 setup. The control link between main optical unit and instrument software, implemented as a CAN-bus, enables the power controller to receive temperature requests. The main control of temperature is assumed by the power controller, which gives a feedback to the instrument software when the temperature stability criteria are reached. The power controller is equipped with a BasicTiger® microcontroller purchased from Wilke (Aachen, Germany), which communicates with the cryostat to set and monitor the temperature of the heat-exchanging fluid; monitoring the temperature of the sample cell was as well by a Pt100 temperature sensor. Finally, the microcontroller is regulating the power supply of the TEM. Due to the requirements of the TEM, the power supply needs to be constant with fixed voltage (4.6 V) and current (3.8 A). For adjustment of TEM power rating, a pulse width modulation at a fixed frequency of 1 kHz is applied. The TEM is used to heat or to cool by reversal of the supply voltages polarity.

Control algorithm

The controlling algorithm is implemented as software in the microcontroller. In comparison to hardware regulators, the software solution is more flexible to adjust the controlling to the circumstances of TEM regulation.

The pulse width is tuned by a self-developed regulation algorithm, which monitors the temperature of the sample cell. The past 60 s of the temperature trend are monitored. Based on these data, the algorithm predicts the temperature to 60 s in the future. The computed "future" temperature is compared with the requested temperature and the TEM power is adjusted proportional to this value.

For precise temperature regulation, it is essential to perform the adjustment on fixed time steps. Due to the performance of the BasicTiger® microcontroller, we recommend a timing of 10 Hz. To take into account the efficiency of the TEM, which

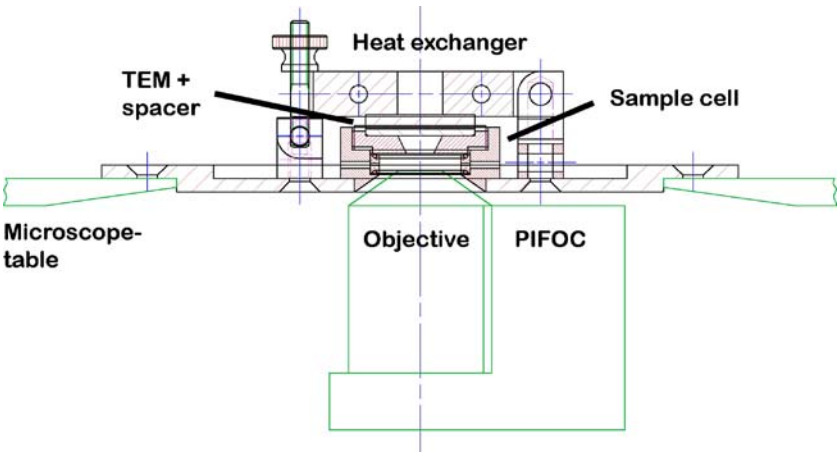

Fig. 2 Assembly of sample environment mounted on a standard microscope table. The heat exchanger is flipped vertically by 90° to open the apparatus for sample change

converts energy loss to heat, an asymmetry factor is included into the regulation algorithm, influencing the proportional adjustment of TEM power.

Temperature calibration

After assembly of the sample cell, the internal Pt100 temperature sensor has to be calibrated. The Pt100 sensor is calibrated in a thermostated water bath, which is monitored with a precession thermometer type GMH 3710 (Greisinger Electronic, Regenstauf, Germany). Because the microscope objective is not temperature-controlled, a temperature offset between the lower body of the sample cell and sample volume is induced. This evokes an additional calibration of the temperature in the sample volume.

Several references for temperature calibration in small confocal volumes can be found. One approach is the measurement of temperature-dependent fluorescence intensity, which occurs on special chemicals like thermochromic liquids [25], Ni(II) high-spin/low-spin interconversion [26], semiconducting nanoparticles [27], or thermoresponsive polymers [28, 29]. Another approach takes the fluorescent lifetime changes of rhodamin B into account [30], which is influenced by conformational changes of sidegroups depending on the chemical environment [31, 32].

To calibrate temperature inside the sample volume, we performed diffusion measurements of TS 100 particles in the range of 5.0 to 65.0 °C with a step width of 2.5 K and 50 repeats for each temperature. Hereof obtained diffusion coefficients and the known R_h of TS 100 (R_h=56.6 nm) are used to calculate solvent viscosity according to the Stokes–Einstein equation (Eq. 5). By this calculation, temperature accuracy is determined to be ±0.1 K.

For temperature stability, we considered that temperature fluctuations inside the sample volume are equal to those in the lower body of the sample cell; monitoring was via the Pt100 sensor, which determined the fluctuations to be below ±0.05 K.

Compensation of thermally induced sample shift

Changing sample temperature leads to a significant and reproducible sample displacement in the *z*-direction. The origin of the displacement is a cumulative effect of thermally induced volume changes of the metal parts of the sample cell, of the Plexiglas® stage, and of the thermally induced change of the refractive index of the sample and immersion water. The contribution of each individual factor was not examined more closely because the entire displacement effect has to be compensated.

This displacement can be monitored by temperature-dependent *x*–*z* imaging of the backscattered light from the surface of a cover glass. Regarding to the point that the working distance of the objective (distance between the top of the objective lens and the focus) is approximately 280 μm with 180 μm thickness of the cover glass, the maximal depth of reachable investigation volume inside the sample has a thickness in the *z*-direction of approximately 100 μm. To achieve precise values, the position error in the *z*-direction should be less than 1% or 1 μm. The importance of position control becomes more obvious by comparing the thermal *z*-displacement, which is shown in Fig. 3, with the acceptance limit of 1 μm. To overcome this problem, an electric actuator for objective positioning was developed.

The mechanical part consists of two stepper motors which are alternatively connected to the manual turning knob of the microscope. One stepper motor is used directly, the other one is equipped with a gearbox, and both are coupled by magnetic clutches. For security reasons, a lower limitation is set by a photoelectric reflex barrier. To guarantee the precise position of the objective relative to the sample, the distance between sample stage and objective piezo controller (PIFOC) is measured with an inductive digital comparator (Millimess Inductive Digital Comparator Extramess 2001, Mahr, Göttingen, Germany).

The power supply is equipped with a BasicTiger® microcontroller and also attached to the system-wide CAN-bus. The calibration curve of objective position versus temperature and the temperature which is associated to zero point is stored in the microcontroller. In the automatic modus, the microcontroller receives the requested temperature from the instrument software and moves the objective with respect to the calibration curve and zero point to the right position. For manual adjustment, the controller is equipped with a control unit for positioning as well as zero point setting.

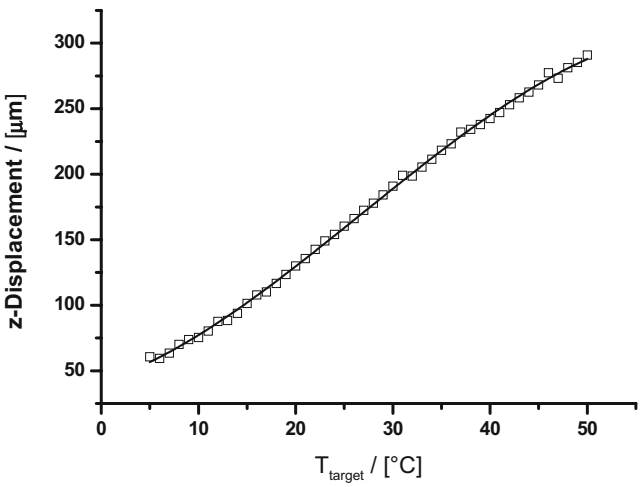

Fig. 3 Thermal displacement of the sample in the *z*-direction between microscope objective and upper surface of lower cover glass in the temperature range of 5.0 to 50.0 °C

Results and discussion

To get precise measurements of diffusion coefficients in 2fFCS experiments, it is absolutely essential to provide exact and reproducible temperatures in the sample cell. Hence, while developing a new kind of temperature-controlled sample cell for 2fFCS experiments, two aspects need to be considered: (1) the time to reach an equilibrated temperature in the setup has to be as short as possible and (2) long-time temperature stability inside the sample has to be ensured. Both criteria are achieved with the sample cell presented in Figs. 1 and 2.

A comparison of target temperature, actual temperature in the sample cell, and temperature of the water bath is shown in Fig. 4, upper plot. After a temperature jump from 20.0 to 25.0 °C, a slight overshoot (15–20% of the temperature difference) in the sample cell temperature is observed. This effect is expected because the temperature sensor is not located in the sample volume itself but outside of it. For the cooling step, the same behavior is observed.

The lower plot of Fig. 4 shows the heating/cooling power which is applied to the TEM. The usable maximal power of ±18 W is used at the beginning of the temperature jump. After the cryostat reaches a constant temperature, the temperature inside the sample is adjusted to the target temperature. The difference between the heating and cooling step can also be seen in this plot. For the heating step, the energy loss of the TEM is added to the energy flow, and for the cooling step the lost energy has to be compensated.

As stated above, the temperature has to be stable over long times. At elevated or deep temperatures, only the heat flux through TEM is changed. At room temperature, the heat flux needs to be constantly inverted, which is a more challenging task for the temperature controller. Due to this, we decided to demonstrate the stability of the sample cell at 25.0 °C, which is shown in Fig. 5. The diffusion coefficient of TS 100 latex particles measured for 10 h at 25.0 °C is presented. As the diffusion coefficient depends on solvent viscosity, which depends itself on temperature (Stokes–Einstein equation), we get a direct correlation. Statistic deviations of diffusion coefficient are smaller than deviations in the 2fFCS experiment itself, which means that temperature, either in the sample cell or in the sample environment, has no influence on the results anymore.

To further examine the capability of the sample cell with respect to absolute temperature and temperature stability, we have investigated a thermoresponsive PNIPAM microgel. Thermosensitive polymers can be customized with respect to particle size and to show a sharp and reversible transition at a well-defined temperature, making these kinds of materials perfect indicators for temperature changes in sample environment [23, 33–36].

The temperature-dependent particle size of the microgel was determined by means of DLS as a common ensemble measurement technique. In the DLS apparatus, the sample is located in a water bath providing a homogenous temperature inside the sample. The temperature is monitored by a calibrated precession thermometer, which allows utilization of measured temperature-dependent hydrodynamic radius of the microgel, as a "quasi" standard for the 2fFCS experiments.

In Fig. 6, we show the correlation functions of the 2fFCS measurement of a microgel below and above the volume phase transition temperature (VPTT). The hydrodynamic

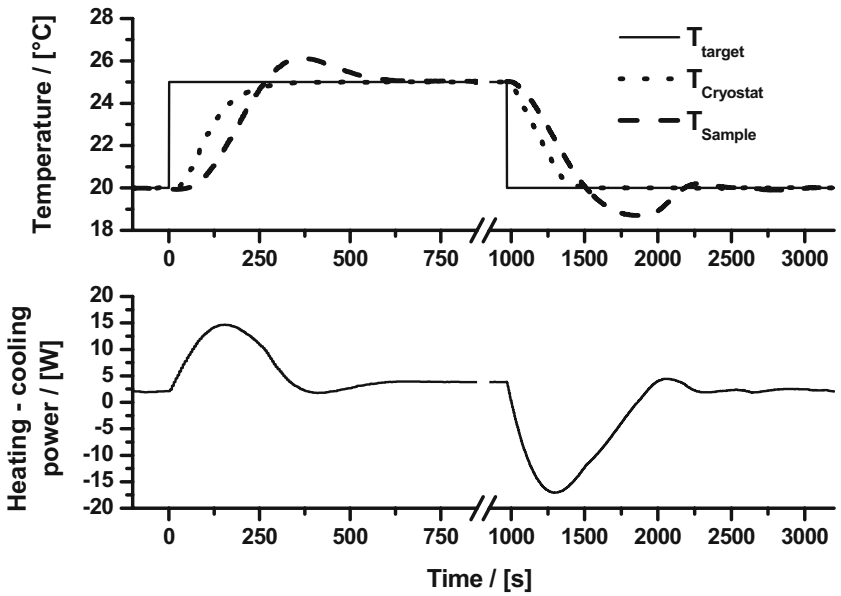

Fig. 4 Temperature jump from 20.0 to 25.0 °C and back. *Upper plot* shows the temperature characteristics of the cryostat and sample cell. *Lower plot* shows the heating/cooling power during the temperature-setting process

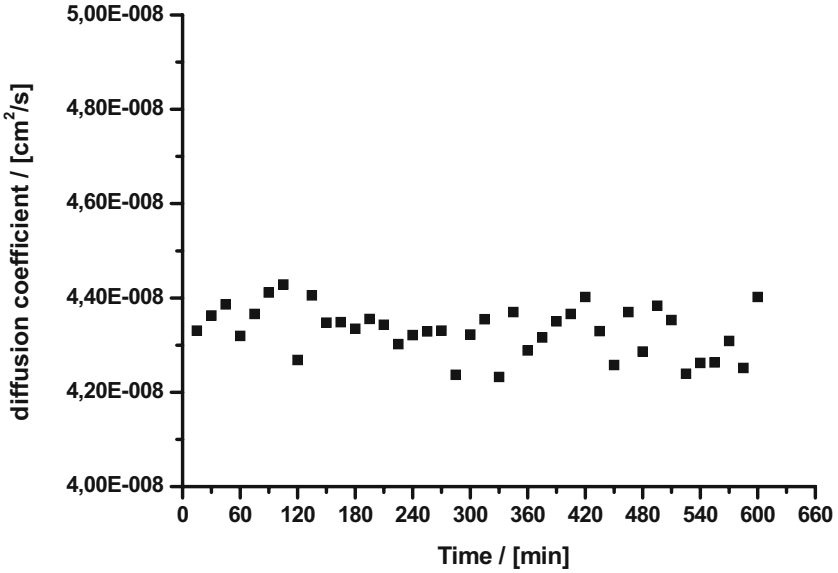

Fig. 5 Diffusion coefficient of TetraSpeck 100-nm fluorescent-labeled latex particles measured 40 times for 15 min each at 25.0 °C

radius was determined from 2fFCS correlation functions by using an enhanced diffusion model for particles with fluorescence distribution within the whole particle [13]. The obtained hydrodynamic radius of 117.2 nm below the VPTT (at 31.2 °C) and 55.9 nm above VPTT (at 36.1 °C) shows a very good agreement with DLS measurement (122.9 nm at 31.0 °C and 56.9 nm at 36.0 °C), which is presented in Fig. 6, inset. The results demonstrate that the temperature controller provides absolute temperature accuracy in the confocal volume of ±0.1 K with a precession of ±0.05 K.

Conclusions

In many studies of biological and colloid samples employing confocal microscopy experiments at elevated temperatures, it is common to heat the samples via a heated objective. This

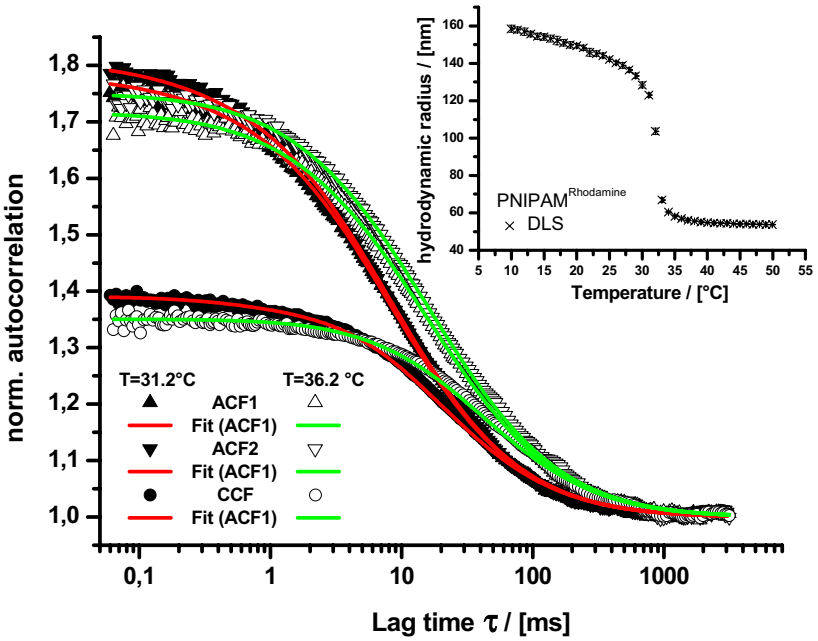

Fig. 6 *Main picture*, 2fFCS curves of a thermoresponsive microgel at two different temperatures. Autocorrelation function (*ACF*) and 2f-cross-correlation function (*CCF*) fitted with enhanced 2fFCS model for multiple-labeled particles. *Inset*, temperature-dependent hydrodynamic radius obtained from DLS

kind of setup is not possible in 2fFCS because mass inertia has to be small for objective scanning techniques. An ideal case would be to control the temperature of the sample cell as well as of the objective because the setup would then be in thermal equilibrium. In this contribution, we show that a special design of the sample cell makes heating of the objective dispensable. Long-time stability experiments over 10 h at 25.0 °C showed that temperature fluctuations in the sample cell are smaller than the experimental resolution of 2fFCS. The new sample cell enables one to measure diffusion coefficients in a broad temperature range with an absolute temperature accuracy of ±0.1 K. This sample cell will provide new opportunities for the investigation of temperature-sensitive polymers and colloids.

Acknowledgements We are much obliged to J. Enderlein for his support of our work. We are indebted to PicoQuant (Berlin, Germany) and Wilke (Aachen, Germany) for the technical support. The financial support by the Deutsche Forschungsgemeinschaft (SPP1259) is gratefully acknowledged.

References

1. Dertinger T, Pacheco V, von der Hocht I, Hartmann R, Gregor I, Enderlein J (2007) ChemPhysChem 8(3):433–443
2. Atkins PW (1978) Physical chemistry. Oxford University Press, Oxford
3. Magde D, Elson EL, Webb WW (1974) Biopolymers 13(1):29–61
4. Petrasek Z, Schwille P (2008) Biophys J 94(4):1437–1448
5. Enderlein J, Gregor I, Patra D, Dertinger T, Kaupp UB (2005) ChemPhysChem 6(11):2324–2336
6. Senff H, Richtering W (1999) J Chem Phys 111(4):1705–1711
7. Stieger M, Pedersen JS, Lindner P, Richtering W (2004) Langmuir 20(17):7283–7292
8. Alsayed AM, Islam MF, Zhang J, Collings PJ, Yodh AG (2005) Science 309(5738):1207–1210
9. St. John AN, Breedveld V, Lyon LA (2007) J Phys Chem B 111 (27):7796–7801
10. Crassous JJ, Wittemann A, Siebenbürger M, Schrinner M, Drechsler M, Ballauff M (2008) Colloid Polym Sci 286:805–812
11. Bonne TB, Papadakis CM, Lüdtke K, Jordan R (2007) Colloid Polym Sci 285(5):491–497
12. Bosco SJ, Zettl H, Crassous JJ, Ballauff M, Krausch G (2006) Macromolecules 39(25):8793–8798
13. Müller CB, Loman A, Richtering W, Enderlein J (2008) J Phys Chem B. doi:10.1021/jp802280u
14. Wong JE, Müller CB, Laschewsky A, Richtering W (2007) J Phys Chem B 111(29):8527–8531
15. Gao Y, Reischmann S, Huber J, Hanke T, Bratschitsch R, Leitenstorfer A, Mecking S (2008) Colloid Polym Sci. doi:10.1007/s00396-008-1899-6
16. Cohen Stuart M (2008) Colloid Polym Sci 286:855–864
17. Guo X, Lu T, Huang X (2008) Colloid Polym Sci 286(4):469–473
18. Nagao D, Yokoyama M, Saeki S, Kobayashi Y, Konno M (2008) Colloid Polym Sci 286:959–964
19. Wahl M, Gregor I, Patting M, Enderlein J (2003) Opt Express 11 (26):3583–3591
20. Müller CB, Weiß K, Richtering W, Loman A, Enderlein J (2008) Opt Express 16(6):4322–4329
21. Einstein A, Fürth R (1956) Investigations on the theory of the Brownian movement. Dover, New York, p p 119
22. Pelton RH, Chibante P (1986) Colloids Surf 20(3):247–256
23. Pelton R (2000) Adv Colloid Interface Sci 85(1):1–33
24. Senff H, Richtering W (2000) Colloid Polym Sci 278(9):830–840
25. Hoang VN, Kaigala GV, Backhouse CJ (2008) Lab Chip 8 (3):484–487
26. Engeser M, Fabbrizzi L, Licchelli M, Sacchi D (1999) Chem Commun (13):1191–1192
27. Wang SP, Westcott S, Chen W (2002) J Phys Chem B 106 (43):11203–11209
28. Iwai K, Matsumura Y, Uchiyama S, de Silva AP (2005) J Mater Chem 15(27–28):2796–2800
29. Uchiyama S, Matsumura Y, de Silva AP, Iwai K (2004) Anal Chem 76(6):1793–1798
30. Benninger RKP, Koc Y, Hofmann O, Requejo-Isidro J, Neil MAA, French PMW, deMello AJ (2006) Anal Chem 78(7):2272–2278
31. Ishizaka S, Kitamura N (2001) Bull Chem Soc Jpn 74(11):1983–1998
32. Kitamura N, Hosoda Y, Iwasaki C, Ueno K, Kim HB (2003) Langmuir 19(20):8484–8489
33. Lutz JF, Akdemir O, Hoth A (2006) J Am Chem Soc 128 (40):13046–13047
34. Keerl M, Richtering W (2007) Colloid Polym Sci 285(4):471–474
35. Huber S, Jordan R (2008) Colloid Polym Sci 286(4):395–402
36. Blackburn W, Lyon L (2008) Colloid Polym Sci 286(5):563–569